NASA TECHNICAL NOTE

NASA TN D-2980

HEAT TRANSFER IN THERMAL ENTRANCE REGION WITH LAMINAR SLIP FLOW BETWEEN PARALLEL PLATES AT UNEQUAL TEMPERATURES

by Robert M. Inman

Lewis Research Center
Cleveland, Ohio

NATIONAL AERONAUTICS AND SPACE ADMINISTRATION • WASHINGTON, D. C. • SEPTEMBER 1965

NASA TN D-2980

HEAT TRANSFER IN THERMAL ENTRANCE REGION WITH LAMINAR SLIP FLOW BETWEEN PARALLEL PLATES AT UNEQUAL TEMPERATURES

By Robert M. Inman

Lewis Research Center
Cleveland, Ohio

NATIONAL AERONAUTICS AND SPACE ADMINISTRATION

For sale by the Clearinghouse for Federal Scientific and Technical Information
Springfield, Virginia 22151 – Price $2.00

HEAT TRANSFER IN THERMAL ENTRANCE REGION WITH LAMINAR SLIP FLOW BETWEEN PARALLEL PLATES AT UNEQUAL TEMPERATURES

by Robert M. Inman

Lewis Research Center

SUMMARY

An analysis was made of the forced-convection heat-transfer characteristics for fully developed incompressible laminar flow between parallel walls with unequal temperatures under the condition that the gas density is low enough to permit a velocity slip and a temperature jump at the walls. The results apply along the entire length of the channel. The solutions contain series expansions and analytical expressions for the complete sets of eigenvalues and eigenfunctions. The results give the wall heat-flux requirements and Nusselt numbers for various values of the rarefaction parameters and dimensionless entrance-temperature parameter. The results show that, in general, the slip-flow heat-flux requirements and Nusselt numbers are lower than those for continuum flow and that they decrease with increased mean free path. The case of slip flow between parallel plates at equal temperatures is included for comparison; the length of duct necessary to obtain a fully developed Nusselt number is, for a given mean free path, the shortest for this case.

INTRODUCTION

The interest in the fluid-mechanics and heat-transfer characteristics of slightly rarefied gases flowing in conduits has been increased in recent years by the advances in high-vacuum technology and by the practical realization of flight at very high altitudes. At normal gas pressures the molecular mean-free-path length is so small that it is possible to consider the behavior of the gas in a conduit by means of well-established theories of continuum fluid mechanics and heat transfer, with the gas adjacent to a surface assuming the velocity and temperature of the surface. At reduced pressures, on the other hand, such as might occur in a vacuum application, the gas flow may take place at a density low enough to permit a velocity slip and a corresponding temperature jump at the conduit wall. This density regime is called the regime of slip flow, and it is this

regime with which the present investigation is concerned. In this regime the molecular mean-free-path length is still small but not negligible.

The problem of laminar continuum flow between parallel flat plates with different temperatures prescribed along each of the two walls is considered in references 1 to 4. Heat transfer for laminar slip flow in a parallel-plate channel with constant wall temperatures is studied in reference 5. The results allow for both walls at the same temperature or else a uniform temperature at one wall and insulation at the other.

Specific consideration is given herein to the heat transfer with laminar, incompressible, fully developed slip flow between a pair of parallel plates, the temperatures of which are maintained constant but not equal. A flat-duct heat exchanger, for example, which heats or cools a gas passing through it may be in contact with a constant temperature bath at each plate. Since the baths are, however, at different temperatures, they thereby maintain the duct walls at constant but unequal temperatures. Another example of channel flow with constant but unequal wall temperatures arises when different coolants undergoing a change of phase are so employed in adjacent flow passages that the temperature of one plate of the gas flow channel differs from that of the other plate. Such exchanger channels are customarily made with small wall thickness and of material with high thermal conductivity, so that a wall is very nearly at a uniform temperature.

The present analysis requires the calculation of the odd eigenvalues and eigenconstants for laminar slip flow. The complete solution is then obtained by combining these odd quantities with the even eigenvalues and eigenconstants that have been determined in reference 5 for slip flow of a rarefied gas between two parallel plates with both walls at the same temperature.

Since the convective term in the energy equation involves the velocity distribution, the first step in the analysis is to specify the velocity over the channel cross section. The fully developed gas velocity distribution for laminar slip flow in a parallel-plate channel was investigated in reference 6, and the results are used in the present study. With the velocity distribution specified, the energy equation can be considered. The solution involves series expansions, and asymptotic analytical expressions are derived for the eigenvalues and eigenconstants as functions of the gas rarefaction parameters and entrance-temperature parameter. Numerical solutions of these quantities are also obtained, and the two methods of computation are compared.

ANALYSIS

A schematic diagram of the parallel-plate channel showing dimensional nomenclature and coordinates is shown in figure 1. The direction of the gas flow is from left to right. For $x < 0$ the plates and the gas are assumed to be isothermal at temperature t_e,

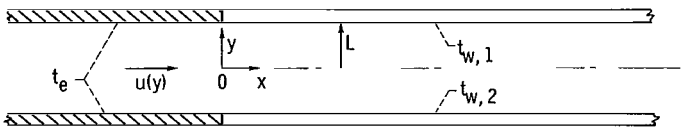

Figure 1. - Physical model and coordinate system for parallel-plate channel.

whereas for $x \geq 0$ the upper plate temperature is step-changed to the constant value $t_{w,1}$ while the lower plate temperature is step-changed to the constant value $t_{w,2}$. (All symbols are defined in appendix A.) Each plate surface is characterized by a pair of properties, the thermal accommodation coefficient a and the reflection coefficient σ (ref. 7). In general, a and σ may be different for each surface; for the present study, however, it will be assumed that $a_1 = a_2 \equiv a$ and that $\sigma_1 = \sigma_2 \equiv \sigma$. Throughout the analysis, the gas flow is assumed hydrodynamically fully developed, viscous dissipation and axial conduction are neglected compared with the conduction in the transverse y-direction, fluid properties are assumed constant, and interactions between the velocity and temperature fields, such as thermal creep, are neglected. It is desired to determine the wall heat-flux distribution and the variation in the heat-transfer coefficient at each plate along the entire length of the channel.

Energy Equation

The starting point of the analysis is the differential equation for convective heat transfer in the parallel-plate channel flow and is

$$\rho c_p u \frac{\partial t}{\partial x} = \kappa \frac{\partial^2 t}{\partial y^2} \tag{1}$$

The dimensionless velocity distribution $u/\bar{u}$, where $\bar{u}$ is the average velocity, is obtained from reference 6 and is given by

$$\frac{u(\eta)}{\bar{u}} \equiv f(\eta) = \frac{3}{2} \frac{(1 - \eta^2 + 4\alpha)}{1 + 6\alpha} \tag{2a}$$

$$\frac{u_s}{\bar{u}} = f(1) = \frac{6\alpha}{1 + 6\alpha} \tag{2b}$$

where $\alpha \equiv \xi_u/2L$. The slip coefficient ξ_u is given by the expression (ref. 7)

$$\xi_u = \frac{2 - \sigma}{\sigma} \ell \tag{3}$$

where σ is the reflection coefficient and ℓ is the mean free path:

$$\ell = \sqrt{\frac{\pi}{2}} \frac{\mu \sqrt{R_g t}}{p} \tag{4}$$

Equation (1), with u given by equation (2a), is to be solved subject to appropriate boundary conditions. Two conditions are obtained upon consideration of the effect of gas rarefaction on the thermal boundary condition at the two walls, which permit a jump between the wall temperature t_w and the adjacent gas temperature t_g (ref. 7):

$$t_{g,1} - t_{w,1} = -2 \frac{\xi_t}{2L} \left(\frac{\partial t}{\partial \eta} \right)_{\eta=1} \qquad \text{at } \eta = 1,\ x \geq 0 \tag{5a}$$

$$t_{g,2} - t_{w,2} = 2 \frac{\xi_t}{2L} \left(\frac{\partial t}{\partial \eta} \right)_{\eta=-1} \qquad \text{at } \eta = -1,\ x \geq 0 \tag{5b}$$

where ξ_t represents a temperature-jump coefficient related to other properties of the system by

$$\xi_t = \frac{2 - a}{a} \frac{2\lambda}{\lambda + 1} \frac{\ell}{Pr} \tag{6}$$

The third boundary condition is a specified gas entrance temperature:

$$t = t_e \qquad \text{at } x = 0,\ -1 \leq \eta \leq 1 \tag{7}$$

Equations (1), (5), and (7) may be expressed in terms of nondimensional quantities as

$$f(\eta) \frac{\partial T}{\partial \zeta} = \frac{\partial^2 T}{\partial \eta^2} \tag{8}$$

$$T \equiv T_{g,1} = 1 - 2\Gamma \left(\frac{\partial T}{\partial \eta} \right)_{\eta=1} \qquad \text{at } \eta = 1,\ \zeta \geq 0 \tag{9a}$$

$$T \equiv T_{g,2} = -\left[1 - 2\Gamma \left(\frac{\partial T}{\partial \eta} \right)_{\eta=-1} \right] \qquad \text{at } \eta = -1,\ \zeta \geq 0 \tag{9b}$$

$$T \equiv T_e \quad \text{at} \quad \zeta = 0, \ -1 \leq \eta \leq 1 \tag{9c}$$

where

$$T \equiv \frac{t - t_{w,m}}{t_{w,1} - t_{w,m}} \tag{10}$$

$$T_{g,1} \equiv \frac{t_{g,1} - t_{w,m}}{t_{w,1} - t_{w,m}} \tag{11}$$

$$T_{g,2} \equiv \frac{t_{g,2} - t_{w,m}}{t_{w,1} - t_{w,m}} \tag{12}$$

$$T_e \equiv \frac{t_e - t_{w,m}}{t_{w,1} - t_{w,m}} \tag{13}$$

and

$$\Gamma \equiv \xi_t / 2L$$

If a solution for T that will apply over the entire length of the channel is to be obtained, it is convenient to break T into the sum of two parts. The first part is $T_d \equiv (t_d - t_{w,m})/(t_{w,1} - t_{w,m})$, the fully developed solution, which applies far down the channel from the entrance. The second part is $T^* \equiv (t - t_d)/(t_{w,1} - t_{w,m})$, which is an entrance-region solution that is added to T_d to obtain dimensionless distributions in the region near the entrance of the channel. The dimensionless temperature distributions throughout the channel are given by

$$T = T_d + T^* \tag{14}$$

Fully Developed Solution

Far from the entrance to the channel, the gas temperature is independent of ζ; that is, it is a function of η and the gas rarefaction parameters only, and equation (8) yields

$$\frac{\partial^2 T_d}{\partial \eta^2} = 0 \tag{15}$$

The solution of equation (15) is $T_d = A\eta + B$, where A and B are constants. This result indicates that the temperature is linear across the channel. The boundary conditions are obtained from equations (9) as

$$T_d(1) = 1 - 2\Gamma\left(\frac{\partial T_d}{\partial \eta}\right)_{\eta=1} \tag{16a}$$

$$T_d(-1) = -\left[1 - 2\Gamma\left(\frac{\partial T_d}{\partial \eta}\right)_{\eta=-1}\right] \tag{16b}$$

For the fully developed situation, the boundary condition at the entrance of the heated channel ($\zeta = 0$) need not be considered, since it is accounted for by the entrance region solution. When equations (16) are used, the fully developed solution becomes

$$T_d = \frac{1}{1 + 2\Gamma}\,\eta \tag{17}$$

Entrance Region Solution

If the solution in the thermal entrance region is to be determined, the function T^* is needed. The function T^* must satisfy the equation

$$f(\eta)\,\frac{\partial T^*}{\partial \zeta} = \frac{\partial^2 T^*}{\partial \eta^2} \tag{18}$$

with the boundary conditions

$$T^*(1) = -2\Gamma\left(\frac{\partial T^*}{\partial \eta}\right)_{\eta=1} \qquad \text{at } \eta = 1,\ \zeta > 0 \tag{19a}$$

$$T^*(-1) = 2\Gamma\left(\frac{\partial T^*}{\partial \eta}\right)_{\eta=-1} \qquad \text{at } \eta = -1,\ \zeta > 0 \tag{19b}$$

At $\zeta = 0$, the condition is

$$T(0,\eta) = T_e = T_d(\eta) + T^*(0,\eta)$$

or, by rearranging,

$$T^*(0,\eta) = T_e - \frac{1}{1+2\Gamma}\eta \qquad \text{at } \zeta = 0,\ -1 \leq \eta \leq 1 \tag{19c}$$

A solution to equation (18) may be obtained by the use of the separation-of-variable method, whereby T^* is taken in the form of a product $T^* = X(\zeta)H(\eta)$, where X is a function of ζ alone and H is a function of η alone. Substitution into the differential equation (18) shows that

$$X = e^{-\psi\zeta} \tag{20}$$

$$\frac{d^2H}{d\eta^2} + \psi f(\eta)H = 0 \tag{21a}$$

From equations (19), the boundary conditions on equation (21a) are

$$\left.\begin{aligned} H(1) &= -2\Gamma\left(\frac{dH}{d\eta}\right)_{\eta=1} \\ H(-1) &= 2\Gamma\left(\frac{dH}{d\eta}\right)_{\eta=-1} \end{aligned}\right\} \tag{21b}$$

Equations (21) comprise an eigenvalue problem of the Sturm-Liouville type. Solutions fitting the boundary conditions can be found only for discrete values of ψ, that is, $\psi_1, \psi_2 \ldots \psi_n$, termed eigenvalues. The solutions $H_1, H_2 \ldots H_n$ are the corresponding eigenfunctions. Hence, the solution for T^* can be written as

$$T^* = \sum_{n=1}^{\infty} G_n H_n(\eta) e^{-\psi_n \zeta} \tag{22}$$

The eigenfunctions H_n are treated as functions of η, although, strictly speaking, they

are functions of both η and the eigenvalues ψ_n.

The constants G_n in equation (22) are evaluated to satisfy the condition at the entrance to the heated channel ($\zeta = 0$). Evaluating equation (22) at $\zeta = 0$ and equating the result with equation (19c) gives

$$\sum_{n=1}^{\infty} G_n H_n(\eta) = T^*(0,\eta) = T_e - \frac{1}{1+2\Gamma}\eta \tag{23a}$$

It follows immediately from the properties of the Sturm-Liouville system that

$$G_n = \frac{\int_{-1}^{1}\left(T_e - \frac{1}{1+2\Gamma}\eta\right)f(\eta)H_n(\eta)d\eta}{\int_{-1}^{1} f(\eta)H_n^2(\eta)d\eta} = \frac{T_e\int_{-1}^{1} f(\eta)H_n(\eta)d\eta}{\int_{-1}^{1} f(\eta)H_n^2(\eta)d\eta}$$

$$- \frac{1}{1+2\Gamma}\frac{\int_{-1}^{1}\eta f(\eta)H_n(\eta)d\eta}{\int_{-1}^{1} f(\eta)H_n^2(\eta)d\eta} \tag{23b}$$

Because of the symmetry of $f(\eta)$ about the passage centerline, the eigenfunctions may be even or odd in η. If H_n is an even function, the second term of equation (23b) disappears, while if H_n is an odd function, the first term disappears. Hence, the constants G_n divide into two classes a_n and b_n that are given by the results

$$a_n = \frac{T_e\int_{-1}^{1} f(\eta)Y_n(\eta)d\eta}{\int_{-1}^{1} f(\eta)Y_n^2(\eta)d\eta} = \frac{T_e\int_{0}^{1} f(\eta)Y_n(\eta)d\eta}{\int_{0}^{1} f(\eta)Y_n^2(\eta)d\eta} \tag{24}$$

$$b_n = -\frac{\frac{1}{1+2\Gamma}\int_{-1}^{1}\eta f(\eta)Z_n(\eta)d\eta}{\int_{-1}^{1} f(\eta)Z_n^2(\eta)d\eta} = -\frac{\frac{1}{1+2\Gamma}\int_{0}^{1}\eta f(\eta)Z_n(\eta)d\eta}{\int_{0}^{1} f(\eta)Z_n^2(\eta)d\eta} \tag{25}$$

where $Y_n(\eta)$ and $Z_n(\eta)$ are even and odd functions, respectively; that is, $Y_n(-\eta) = Y_n(\eta)$ and $Z_n(-\eta) = -Z_n(\eta)$. The corresponding eigenvalues are denoted by β_n and γ_n, and the solution for T^* can be rewritten as

$$T^*(\xi, \eta) = \sum_{n=1}^{\infty} a_n Y_n(\eta) e^{-\beta_n \xi} + \sum_{n=1}^{\infty} b_n Z_n(\eta) e^{-\gamma_n \xi} \tag{26}$$

In reference 5 the result for the coefficients a_n, when divided by the wall-temperature parameter T_e, is shown to reduce to

$$a_n' \equiv \frac{a_n}{T_e} = \frac{\int_0^1 f(\eta) Y_n(\eta) d\eta}{\int_0^1 f(\eta) Y_n^2(\eta) d\eta} = - \frac{1}{\beta_n \left(\frac{\partial Y}{\partial \beta} + 2\Gamma \frac{\partial^2 Y}{\partial \eta \, \partial \beta} \right)_{\eta=1;\, \beta=\beta_n}} \tag{27}$$

The series coefficients a_n are thus

$$a_n = - \frac{T_e}{\beta_n \left(\frac{\partial Y}{\partial \beta} + 2\Gamma \frac{\partial^2 Y}{\partial \eta \, \partial \beta} \right)_{\eta=1;\, \beta=\beta_n}} \tag{28}$$

This result implies that once the eigenfunctions $Y_n(\eta; \beta_n)$ are known, the coefficients a_n of equation (28) may be evaluated for a given value of T_e, for example, $T_e = 1$. For other values of T_e, it is only necessary to multiply a_n (for $T_e = 1$) by the new value of T_e to obtain the new coefficients.

As shown in detail in appendix B, the integral appearing in the numerator of equation (25) may be written as

$$\int_0^1 \eta f(\eta) Z_n(\eta) d\eta = - \frac{1 + 2\Gamma}{\gamma_n} \left(\frac{dZ_n}{d\eta} \right)_{\eta=1} \tag{29a}$$

whereas the denominator of equation (25) becomes

$$\int_0^1 f(\eta)Z_n^2(\eta)d\eta = \left(\frac{\partial Z}{\partial \gamma} + 2\Gamma \frac{\partial^2 Z}{\partial \eta \partial \gamma}\right)_{\eta=1;\, \gamma=\gamma_n} \left(\frac{dZ_n}{d\eta}\right)_{\eta=1} \tag{29b}$$

Then, the series coefficients b_n are

$$b_n = \frac{1}{\gamma_n \left(\frac{\partial Z}{\partial \gamma} + 2\Gamma \frac{\partial^2 Z}{\partial \eta \partial \gamma}\right)_{\eta=1;\, \gamma=\gamma_n}} \tag{30}$$

Now that T_d and T^* are known, they can be superposed as in equation (14) to obtain the solution that applies over the entire length of the channel, which is

$$T = \frac{1}{1 + 2\Gamma}\eta + \sum_{n=1}^{\infty} a_n Y_n(\eta) e^{-\beta_n \zeta} + \sum_{n=1}^{\infty} b_n Z_n(\eta) e^{-\gamma_n \zeta} \tag{31}$$

Wall Heat Fluxes

When the wall temperatures are specified, the wall heat-flux variations along the channel length required to maintain the wall temperatures constant are of practical interest. If a sign convention is adopted to give positive heat-transfer rates at both walls for $\zeta \to \infty$, then the heat-transfer rate from the upper wall to the gas is given by

$$q_{w,1} = \kappa \left(\frac{\partial t}{\partial y}\right)_{y=L} = \frac{\kappa}{L}(t_{w,1} - t_{w,m})\left(\frac{\partial T}{\partial \eta}\right)_{\eta=1} \tag{32}$$

and from the gas to the lower wall by

$$q_{w,2} = \frac{\kappa}{L}(t_{w,1} - t_{w,m})\left(\frac{\partial T}{\partial \eta}\right)_{\eta=-1} \tag{33}$$

The heat-transfer rates $q_{w,1}$ and $q_{w,2}$ can be found by differentiating equation (31) with respect to η and evaluating the result at $\eta = 1$ and at $\eta = -1$ to obtain

$$\frac{q_{w,1}L}{\kappa(t_{w,1} - t_{w,m})} = \frac{1}{1 + 2\Gamma} + \sum_{n=1}^{\infty} a_n \left(\frac{dY_n}{d\eta}\right)_{\eta=1} e^{-\beta_n \zeta} + \sum_{n=1}^{\infty} b_n \left(\frac{dZ_n}{d\eta}\right)_{\eta=1} e^{-\gamma_n \zeta} \tag{34}$$

$$\frac{q_{w,2}L}{\kappa(t_{w,1} - t_{w,m})} = \frac{1}{1 + 2\Gamma} - \sum_{n=1}^{\infty} a_n \left(\frac{dY_n}{d\eta}\right)_{\eta=1} e^{-\beta_n \zeta} + \sum_{n=1}^{\infty} b_n \left(\frac{dZ_n}{d\eta}\right)_{\eta=1} e^{-\gamma_n \zeta} \tag{35}$$

since

$$\left(\frac{dY_n}{d\eta}\right)_{\eta=1} = -\left(\frac{dY_n}{d\eta}\right)_{\eta=-1}$$

and

$$\left(\frac{dZ_n}{d\eta}\right)_{\eta=1} = \left(\frac{dZ_n}{d\eta}\right)_{\eta=-1}$$

Equations (34) and (35) indicate that the heat-transfer rates $q_{w,1}$ and $q_{w,2}$ become uniform and equal along the length of the duct after the development length, that is, after the influence of the eigenfunctions dies away.

Nusselt Numbers

In continuum heat-transfer theory, it is customary to represent the heat-transfer results in terms of a heat-transfer coefficient $h \equiv q_w/(t_w - t_b)$ and a Nusselt number $Nu \equiv hD_T/\kappa$, where D_T is the thermal diameter and defined as

$$D_T \equiv 4 \frac{\text{Cross-sectional area}}{\text{Heated perimeter}}$$

For the flat duct, $D_T = 4L$. The extension of these concepts to low-density flows is quite natural and appropriate.

The Nusselt number for the upper wall may be written

$$Nu_1 = \frac{q_{w,1}}{t_{w,1} - t_b} \frac{4L}{\kappa} \tag{36}$$

where t_b, the mixed-mean temperature of the gas, is given by

$$t_b = \frac{\int_{-1}^{1} ut \, d\eta}{\int_{-1}^{1} u \, d\eta} = \frac{1}{2} \int_{-1}^{1} f(\eta) t \, d\eta \tag{37}$$

since

$$\int_{-1}^{1} u \, d\eta = 2\bar{u}$$

The Nusselt number Nu_1 may be expressed alternatively as

$$Nu_1 = \frac{4}{1 - T_b} \left(\frac{\partial T}{\partial \eta} \right)_{\eta=1} \tag{38}$$

where

$$T_b = \frac{t_b - t_{w,m}}{t_{w,1} - t_{w,m}} = \frac{1}{2} \int_{-1}^{1} f(\eta) T \, d\eta \tag{39}$$

The Nusselt number at the lower wall may be written in the same manner as

$$Nu_2 = \frac{q_{w,2}}{t_b - t_{w,2}} \frac{4L}{\kappa} \tag{40}$$

and hence

$$Nu_2 = \frac{4}{1 + T_b} \left(\frac{\partial T}{\partial \eta} \right)_{\eta=-1} \tag{41}$$

Putting equations (38) and (41) into more useful forms necessitates knowing the dimensionless bulk temperature T_b, given by equation (39). Introducing the temperature distribution (eq. (31)) and the velocity distribution (eq. (2a)) into equation (39) yields

$$T_b = \frac{1}{2}\sum_{n=1}^{\infty} a_n e^{-\beta_n \zeta} \int_{-1}^{1} f(\eta) Y_n \, d\eta + \frac{1}{2}\sum_{n=1}^{\infty} b_n e^{-\gamma_n \zeta} \int_{-1}^{1} f(\eta) Z_n \, d\eta \tag{42}$$

The first integral on the right side of equation (42) can be evaluated by using equation (21a) for an even eigenfunction with the result

$$\int_{-1}^{1} f(\eta) Y_n \, d\eta = 2 \int_{0}^{1} f(\eta) Y_n \, d\eta = -\frac{2}{\beta_n} \int_{0}^{1} \frac{d^2 Y_n}{d\eta^2} \, d\eta = -\frac{2}{\beta_n} \left(\frac{dY_n}{d\eta}\right)_0^1 = -\frac{2}{\beta_n} \left(\frac{dY_n}{d\eta}\right)_{\eta=1}$$

since $(dY_n/d\eta)_{\eta=0} = 0$ by symmetry, while the second integral in equation (42) reduces to zero, since integrals of odd functions from $\eta = 1$ to $\eta = -1$ are zero. With these results, equation (42) becomes

$$T_b = -\sum_{\eta=1}^{\infty} \frac{a_n}{\beta_n} \left(\frac{\partial Y_n}{\partial \eta}\right)_{\eta=1} e^{-\beta_n \zeta} \tag{43}$$

Final expressions for the Nusselt numbers may be written, with the use of equations (32) to (35), (38), (41), and (43), as

$$Nu_1 = \frac{\dfrac{1}{1+2\Gamma} + \displaystyle\sum_{n=1}^{\infty} a_n \left(\frac{\partial Y_n}{\partial \eta}\right)_{\eta=1} e^{-\beta_n \zeta} + \sum_{n=1}^{\infty} b_n \left(\frac{\partial Z_n}{\partial \eta}\right)_{\eta=1} e^{-\gamma_n \zeta}}{\dfrac{1}{4} + \dfrac{1}{4}\displaystyle\sum_{n=1}^{\infty} \frac{a_n}{\beta_n} \left(\frac{\partial Y_n}{\partial \eta}\right)_{\eta=1} e^{-\beta_n \zeta}} \tag{44}$$

$$Nu_2 = \frac{\dfrac{1}{1+2\Gamma} - \displaystyle\sum_{n=1}^{\infty} a_n \left(\frac{\partial Y_n}{\partial \eta}\right)_{\eta=1} e^{-\beta_n \zeta} + \sum_{n=1}^{\infty} b_n \left(\frac{\partial Z_n}{\partial \eta}\right)_{\eta=1} e^{-\gamma_n \zeta}}{\dfrac{1}{4} - \dfrac{1}{4}\displaystyle\sum_{n=1}^{\infty} \frac{a_n}{\beta_n} \left(\frac{\partial Y_n}{\partial \eta}\right)_{\eta=1} e^{-\beta_n \zeta}} \tag{45}$$

Equations (44) and (45) give the Nusselt number variation for each wall along the entire length of the duct. The fully developed value for the Nusselt numbers is obtained when $\zeta \to \infty$ and is the same for both walls:

$$Nu_{1,d} = Nu_{2,d} = \frac{4}{1+2\Gamma} \tag{46}$$

Hence, it is necessary for the influence of all eigenfunctions (odd and even) to die away before this condition is reached. The fully developed condition also yields the linear temperature profile given by equation (17):

$$T_d = \frac{1}{1+2\Gamma}\eta \tag{17}$$

which remains unchanged at any value of ζ from this point on. In the corresponding case with equal wall temperatures, the Nusselt number becomes fully developed when the temperature profiles at different distances from the entrance become similar, that is, when the value of ζ is sufficiently large for the influence of the second and higher even eigenfunctions to be negligible (ref. 5). This similarity occurs at distances which are much shorter than those in the unsymmetrical case. In addition, the fully developed condition in the case of unsymmetrical wall temperatures corresponds to the condition where there is no net heat transfer to the fluid, whereas in the symmetrical case there is a net heat transfer to or from the fluid. These factors result in (1) a shorter thermal entry length and (2) a higher value of Nu_d for the symmetrical as compared with the unsymmetrical wall temperature case.

Equation (46) indicates that the fully developed Nusselt numbers $Nu_{1,d}$ and $Nu_{2,d}$ are dependent only upon the temperature-jump parameter Γ when the plates are maintained at unequal temperatures. This result differs from that obtained when the wall temperatures are equal (ref. 5). In the latter case, the fully developed Nusselt number was found to depend upon the first eigenvalue given in reference 5, which, in turn, depended upon the two rarefaction parameters α and Γ.

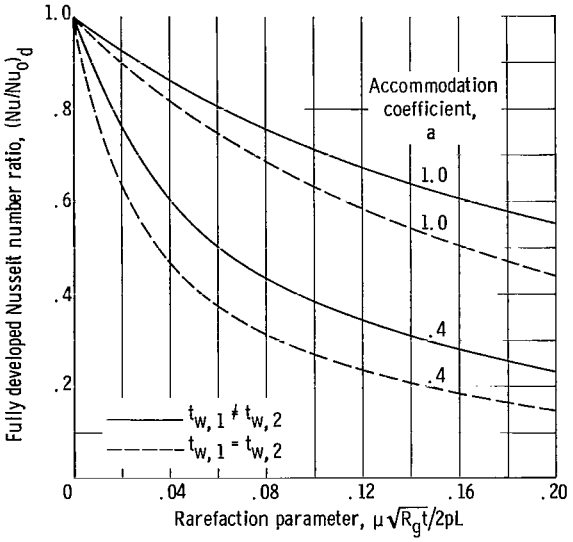

Figure 2. - Fully developed Nusselt number ratio for slip flow in channel. Specular reflection coefficient, 1; ratio of specific heats, 1.4; Prandtl number, 0.73.

Fully developed Nusselt numbers obtained from equation (46) are plotted in figure 2 as a function of $\mu\sqrt{R_g t}/2pL$ in the form of a ratio $(Nu/Nu_0)_d$, where Nu_0 represents the continuum value 4.00. Also shown are fully developed Nusselt numbers for the case of equal wall temperatures (ref. 5), where now $Nu_0 = 7.53$. The effect of gas rarefaction is to decrease the value of the Nusselt number below its continuum value. The effect on the Nusselt number of the specified value of accommodation coefficient is apparent. The effects of gas rarefaction on the fully developed Nusselt number are more pronounced with equal wall temperatures than in the corresponding case with unequal wall temperatures.

Axial Variation of Gas Temperature Adjacent to Wall

The axial variations of the gas temperatures adjacent to the wall are perhaps also of engineering interest. These quantities are obtained readily from equation (31) by setting $\eta = 1$ and $\eta = -1$ therein. The gas temperature adjacent to the upper wall is

$$T(\zeta, 1) = \frac{1}{1 + 2\Gamma} + \sum_{n=1}^{\infty} a_n Y_n(1) e^{-\beta_n \zeta} + \sum_{n=1}^{\infty} b_n Z_n(1) e^{-\gamma_n \zeta} \tag{47a}$$

while that adjacent to the lower wall is

$$T(\zeta, -1) = -\frac{1}{1 + 2\Gamma} + \sum_{n=1}^{\infty} a_n Y_n(1) e^{-\beta_n \zeta} - \sum_{n=1}^{\infty} b_n Z_n(1) e^{-\gamma_n \zeta} \tag{47b}$$

According to equation (21b), however,

$$Y_n(1) = -2\Gamma \left(\frac{\partial Y_n}{\partial \eta}\right)_{\eta=1}$$

$$Z_n(1) = -2\Gamma\left(\frac{\partial Z_n}{\partial \eta}\right)_{\eta=1}$$

Then, equations (47a) and (47b) become, respectively,

$$T(\zeta, 1) = \frac{1}{1 + 2\Gamma} - 2\Gamma\left[\sum_{n=1}^{\infty} a_n\left(\frac{\partial Y_n}{\partial \eta}\right)_{\eta=1} e^{-\beta_n \zeta} + \sum_{n=1}^{\infty} b_n\left(\frac{\partial Z_n}{\partial \eta}\right)_{\eta=1} e^{-\gamma_n \zeta}\right] \tag{48a}$$

$$T(\zeta, -1) = -\frac{1}{1 + 2\Gamma} - 2\Gamma\left[\sum_{n=1}^{\infty} a_n\left(\frac{\partial Y_n}{\partial \eta}\right)_{\eta=1} e^{-\beta_n \zeta} - \sum_{n=1}^{\infty} b_n\left(\frac{\partial Z_n}{\partial \eta}\right)_{\eta=1} e^{-\gamma_n \zeta}\right] \tag{48b}$$

In the absence of a temperature jump ($\Gamma = 0$), it is apparent from equation (48a) that $t_{g,1} = \text{constant} = t_{w,1}$, while from equation (48b) it is seen that for $\Gamma = 0$, $t_{g,2} = t_{w,2}$. With a temperature-jump effect, however, $t_{g,1} \neq t_{w,1}$ and $t_{g,2} \neq t_{w,2}$.

The foregoing expressions indicate that the solution requires the computation of β_n, γ_n, a_n, b_n, $(\partial Y_n/\partial \eta)_{\eta=1}$, and $(\partial Z_n/\partial \eta)_{\eta=1}$. Attention is now directed to the Sturm-Liouville eigenvalue problem (eqs. (21)).

Transverse Distribution Functions $Y(\eta), Z(\eta)$

The even function $Y(\eta)$ is the even solution of equations (21) and the customary normalization convention $Y(0) \equiv 1$. Asymptotic expressions for large values of n for the even eigenvalues β_n and constants $A_n \equiv a_n(\partial Y_n/\partial \eta)_{\eta=1}$ are given in reference 5, and the results are presented herein to make the analysis more complete:

$$\delta_n \tan \delta_n = \frac{(4\alpha + \Gamma)\left[\sqrt{4\alpha} + (1 + 4\alpha)\sin^{-1}\left(\frac{1}{\sqrt{1 + 4\alpha}}\right)\right]}{4\Gamma(4\alpha)^{3/2}} \equiv C \tag{49}$$

$$A_n \equiv a_n\left(\frac{\partial Y_n}{\partial \eta}\right)_{\eta=1} = -\frac{4\alpha T_e}{\Gamma(4\alpha + \Gamma)\left(C + 1 + \frac{\delta_n^2}{C}\right)} \tag{50}$$

where

$$\delta_n \equiv \sqrt{\beta_n} I_1 \tag{51}$$

$$I_1 \equiv \int_0^1 \sqrt{f(\eta)}\, d\eta = \frac{\sqrt{3/8}\left[\sqrt{4\alpha} + (1 + 4\alpha)\sin^{-1}\left(\frac{1}{\sqrt{1 + 4\alpha}}\right)\right]}{\sqrt{1 + 6\alpha}} \tag{52}$$

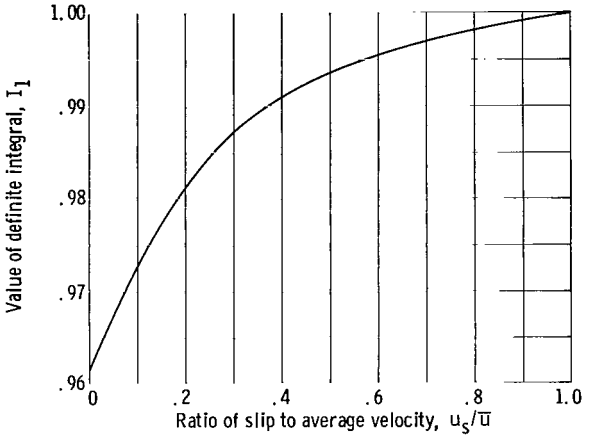

Figure 3. - Value of definite integral for any ratio of slip to average velocity.

The first six roots of equation (49) are given in reference 8 for a number of values of C. The values of I_1 for any given ratio of slip velocity to average velocity $u_s/\bar{u}$ are shown in figure 3.

The odd eigenvalues γ_n and eigenconstants b_n and $(\partial Z_n/\partial\eta)_{\eta=1}$ are determined from the odd solution of equations (21) and the condition $Z(0) = 0$. This latter condition is obtained by setting $\eta = 0$ in the condition $Z(\eta) = -Z(-\eta)$. If the methods presented in reference 5 to determine the asymptotic expressions for large values of n for the case of equal wall temperatures are applied, the asymptotic solution of equations (21) for the odd functions $Z(\eta)$ satisfying the condition $Z(0) = 0$ is

$$Z(\eta) = D(1 + 4\alpha)^{1/4}(1 - \eta^2 + 4\alpha)^{-1/4} \sin(\sqrt{\gamma}\, J) \tag{53}$$

$$\frac{\partial Z}{\partial \eta} = \frac{D}{2}(1+4\alpha)^{1/4}(1-\eta^2+4\alpha)^{-5/4}\left[\eta \sin(\sqrt{\gamma}J) + 4\frac{\sqrt{3/8}\,(1-\eta^2+4\alpha)^{3/2}(\sqrt{\gamma}J)\cos(\sqrt{\gamma}J)}{J\sqrt{1+6\alpha}}\right] \tag{54}$$

where D is an arbitrary constant and

$$J \equiv \int_0^\eta \sqrt{f(\eta)}\, d\eta = \frac{\sqrt{3/8}\left[\eta\sqrt{1 - \eta^2 + 4\alpha} + (1 + 4\alpha)\sin^{-1}\left(\frac{\eta}{\sqrt{1 + 4\alpha}}\right)\right]}{\sqrt{1 + 6\alpha}} \tag{55}$$

The values of the function Z and its slope $dZ/d\eta$ at the upper plate are found by setting $\eta = 1$ in equations (53) and (54), respectively; the results are

$$Z(1) = D\left(\frac{1 + 4\alpha}{4\alpha}\right)^{1/4} \sin \epsilon \tag{56}$$

$$\left(\frac{\partial Z}{\partial \eta}\right)_{\eta=1} = \frac{D}{2}(1 + 4\alpha)^{1/4}(4\alpha)^{-5/4}\left[\sin \epsilon + \frac{2\left(\frac{3}{2}\right)^{1/2}(4\alpha)^{3/2}\epsilon \cos \epsilon}{J_1(1 + 6\alpha)^{1/2}}\right] \tag{57}$$

where

$$\epsilon \equiv \sqrt{\gamma}\, J_1 \tag{58}$$

and

$$J_1 \equiv \int_0^1 \sqrt{f(\eta)}\, d\eta = I_1 \tag{59}$$

The eigenvalues γ_n are determined by the requirement $Z(1) = -2\Gamma(dZ/d\eta)_{\eta=1}$. Then, with equations (56) and (57) combined in accordance with this relation, the eigenvalues are obtained as roots of the characteristic equation

$$\epsilon_n \cot \epsilon_n = -\frac{(4\alpha + \Gamma)\left[\sqrt{4\alpha} + (1 + 4\alpha)\sin^{-1}\frac{1}{\sqrt{1 + 4\alpha}}\right]}{4\Gamma(4\alpha)^{3/2}}$$

$$= -C \tag{60}$$

where $\epsilon_n \equiv \sqrt{\gamma_n}\, J_1$. The first six roots of equation (60) are given in reference 8 for a number of values of C. The eigenfunctions corresponding to these eigenvalues will be denoted by Z_n. From equations (49) and (60) the eigenvalues β_n and γ_n (and hence the eigenfunctions Y_n and Z_n) can be seen to depend on the two rarefaction parameters $\xi_u/2L$ and $\xi_t/2L$.

If the series coefficients b_n (eq. (30)) are to be obtained, it is necessary to evaluate the terms $(\partial Z/\partial\gamma)_{\eta=1;\,\gamma=\gamma_n}$ and $(\partial^2 Z/\partial\eta\,\partial\gamma)_{\eta=1;\,\gamma=\gamma_n}$. These expressions are determined by differentiating equations (56) and (57), respectively, with respect to γ. The results may be written as

$$\left(\frac{\partial Z}{\partial \gamma}\right)_{\eta=1;\,\gamma=\gamma_n} = -\frac{D(1+4\alpha)^{1/4} C \sin \epsilon_n}{2\gamma_n (4\alpha)^{1/4}} \tag{61a}$$

$$\left(\frac{\partial^2 Z}{\partial \eta \partial \gamma}\right)_{\eta=1;\,\gamma=\gamma_n} = -\frac{D(1+4\alpha)^{1/4}\left[C + \dfrac{(4\alpha+\Gamma)\left(C+\epsilon_n^2\right)}{C\Gamma}\right] \sin \epsilon_n}{4\gamma_n (4\alpha)^{5/4}} \tag{61b}$$

Thus, the coefficients b_n as evaluated from equation (30) are given by

$$b_n = -\frac{8\alpha(4\alpha)^{1/4}}{D(4\alpha+\Gamma)(1+4\alpha)^{1/4}\left(C+1+\dfrac{\epsilon_n^2}{C}\right)\sin \epsilon_n} \tag{62}$$

The slope $dZ/d\eta$ evaluated at the wall, given by equation (57), can be alternately expressed as

$$\left(\frac{dZ_n}{d\eta}\right)_{\eta=1} = -\frac{D(1+4\alpha)^{1/4} \sin \epsilon_n}{2\Gamma(4\alpha)^{1/4}} \tag{63}$$

It is convenient to define a new coefficient B_n, given by the product of b_n and $(dZ_n/d\eta)_{\eta=1}$, as

$$B_n \equiv b_n\left(\frac{dZ_n}{d\eta}\right)_{\eta=1} = \frac{4\alpha}{\Gamma(4\alpha+\Gamma)\left(C+1+\dfrac{\epsilon_n^2}{C}\right)} \tag{64}$$

Equations (49), (50), (60), and (64) can be used to calculate the eigenvalues β_n and γ_n and the coefficients A_n and B_n for arbitrarily chosen values of $\xi_u/2L$ or $u_s/\bar{u}$ and $\xi_t/2L$.

The first four values of $\sqrt{\beta_n}$ calculated from the asymptotic expressions together with the corresponding values of A_n are listed in table I as analytical values for several values of the parameters $u_s/\bar{u}$ and $\xi_t/2L$. The first four values of $\sqrt{\gamma_n}$ calculated from the asymptotic expressions together with the corresponding values of B_n are listed in table II as analytical values for these same values of $u_s/\bar{u}$ and $\xi_t/2L$. The

TABLE I. - EVEN EIGENVALUES AND COEFFICIENTS FOR LAMINAR SLIP FLOW IN PARALLEL-PLATE CHANNEL WITH UNEQUAL WALL TEMPERATURES (T_e = 1)

	Ratio of slip to average velocity, $u_s/\bar{u}$							
	1/3				3/5			
	Temperature-jump coefficient, $\xi_t/2L$							
	0.1333		0.5333		0.4		1.6	
	Solution							
	Analytical	Numerical	Analytical	Numerical	Analytical	Numerical	Analytical	Numerical
Eigenvalue								
$\sqrt{\beta_1}$	1.431	1.168	1.289	0.8128	1.111	0.9087	0.8750	0.5273
$\sqrt{\beta_2}$	4.321	4.083	4.010	3.630	3.705	3.602	3.451	3.337
$\sqrt{\beta_3}$	7.265	7.085	6.906	6.682	6.645	6.586	6.475	6.417
$\sqrt{\beta_4}$	10.28	10.14	9.945	9.794	9.700	9.661	9.581	9.541
Coefficient								
$-A_1$	0.5245	1.292	0.1291	0.6532	0.4705	0.8105	0.0869	0.2775
$-A_2$	.4455	.6554	.0808	.1275	.1925	.2077	.0180	.0196
$-A_3$	.3380	.4078	.0441	.0504	.0789	.0797	.00578	.00579
$-A_4$	.2500	.2716	.0255	.0265	.0399	.0401	.00270	.00270

even eigenvalues and coefficients for continuum flow ($\xi_u/2L = \xi_t/2L = 0$) in a channel with unequal wall temperatures are given in table III and were obtained from reference 9, while the odd eigenvalues and coefficients are listed in table IV and were obtained from reference 4.

The level of accuracy for the slip-flow eigenvalues and eigenconstants was checked by solving numerically the Sturm-Liouville equations (21) by means of the Runge-Kutta method on an IBM 7094 digital computer. Reference 5 presents numerical values for the even quantities $\sqrt{\beta_n}$ and A_n calculated in this manner, and the results are given in table I. Equations (21) were solved numerically for the odd quantities in the course of the present investigation. The forward integration was started by using the condition $Z_n(0) = 0$ and by arbitrarily letting $(dZ_n/d\eta)_{\eta=0} = 1$. The eigenvalues were found by trial and error until the boundary condition $Z_n(1) = -2\Gamma(dZ_n/d\eta)_{\eta=1}$ was satisfied at $\eta = 1$. The first four eigenvalues $\sqrt{\gamma_n}$ and coefficients B_n calculated in this manner are given in table II. There is good agreement between the relevant quantities computed from the analytical asymptotic expressions and the numerical solutions even for values of n as

TABLE II. - ODD EIGENVALUES AND COEFFICIENTS FOR LAMINAR SLIP FLOW IN PARALLEL-PLATE CHANNEL WITH UNEQUAL WALL TEMPERATURES

	Ratio of slip to average velocity, $u_s/\bar{u}$							
	1/3				3/5			
	Temperature-jump coefficient, $\xi_t/2L$							
	0.1333		0.5333		0.4		1.6	
	Solution							
	Analytical	Numerical	Analytical	Numerical	Analytical	Numerical	Analytical	Numerical
	Eigenvalue							
$\sqrt{\gamma_1}$	2.871	2.610	2.615	2.163	2.390	2.194	2.051	1.849
$\sqrt{\gamma_2}$	5.780	5.574	5.430	5.144	5.150	5.076	4.950	4.866
$\sqrt{\gamma_3}$	8.755	8.603	8.405	8.232	8.160	8.114	8.025	7.974
$\sqrt{\gamma_4}$	11.79	11.68	11.49	11.36	11.23	11.21	11.12	11.10
	Coefficient							
B_1	0.4925	0.8717	0.1061	0.2503	0.3155	0.3868	0.0398	0.0526
B_2	.3925	.5099	.0598	.0761	.1199	.1231	.00954	.00967
B_3	.2921	.3290	.0348	.0354	.0549	.0547	.00381	.00377
B_4	.2139	.2244	.0206	.0201	.0304	.0298	.00201	.00195

TABLE III. - EVEN EIGENVALUES AND COEFFICIENTS FOR LAMINAR CONTINUUM FLOW IN PARALLEL-PLATE CHANNEL WITH UNEQUAL WALL TEMPERATURES ($T_e = 1$)

[Data from ref. 9.]

Eigenvalue	
$\sqrt{\beta_1}$	1.372
$\sqrt{\beta_2}$	4.625
$\sqrt{\beta_3}$	7.890
$\sqrt{\beta_4}$	11.16
Coefficient	
$-A_1$	1.708
$-A_2$	1.138
$-A_3$	.951
$-A_4$	.848

TABLE IV. - ODD EIGENVALUES AND COEFFICIENTS FOR LAMINAR CONTINUUM FLOW IN PARALLEL-PLATE CHANNEL WITH UNEQUAL WALL TEMPERATURES

[Data from ref. 4.]

Eigenvalue	
$\sqrt{\gamma_1}$	2.992
$\sqrt{\gamma_2}$	6.250
$\sqrt{\gamma_3}$	9.495
$\sqrt{\gamma_4}$	12.78
Coefficient	
B_1	1.319
B_2	1.029
B_3	.894
B_4	.751

low as 3. The extent of agreement depends on the parameters $u_s/\bar{u}$ and $\xi_t/2L$ with the best agreement at low values of $\xi_t/2L$ and higher values of $u_s/\bar{u}$. For those having access to digital or analog computing machines, the analytical expressions may provide helpful check solutions and for those who do not, the expressions presented herein employing a rapidly converging series solution suitable for hand calculations and yielding values that are sufficiently accurate may be a useful tool. Furthermore, it is evident from the comparisons that the analytical expressions have definite application to determining the higher eigenvalues for laminar slip flow heat transfer in channels.

RESULTS AND DISCUSSION

With the numerical information in tables I to IV, the variation along the length of the channel of the wall heat fluxes, Nusselt numbers, and temperature of the gas adjacent to each wall can be evaluated from equations (34) and (35), (44) and (45), and (48a) and (48b), respectively. These quantities also depend on the magnitude of the entrance temperature in relation to the values of the wall temperatures, or on the wall-temperature parameter T_e.

The particular values of the wall-temperature parameter T_e chosen for the computations correspond to the following cases: (a) $T_e = \mp 2$, in which the wall temperatures are unequal but both are maintained at higher or lower temperatures than the temperature of the gas entering the channel; (b) $T_e = \mp 1$, in which the lower wall or upper wall, respectively, is at the temperature of the gas entering the channel; and (c) $T_e = 0$, in which the arithmetic average of the wall temperatures is equal to the temperature of the gas entering the channel (i.e., $(t_{w,1} + t_{w,2})/2 = t_e$).

The last case ($T_e = 0$) is a special case and warrants some additional discussion. For this special case, only odd eigenfunctions are involved in the various quantities of engineering interest (since $a_n = 0$ from eq. (24)), and hence the wall heat-flux variations (eqs. (34) and (35)), bulk temperature (eq. (43)), Nusselt numbers (eqs. (44) and (45)), and temperatures of the gas adjacent to the walls (eqs. (48)) reduce to, respectively,

$$\frac{q_{w,1}L}{\kappa(t_{w,1} - t_{w,m})} = \frac{q_{w,2}L}{\kappa(t_{w,1} - t_{w,m})} = \frac{1}{1 + 2\Gamma} + \sum_{n=1}^{\infty} B_n e^{-\gamma_n \zeta}$$

$$T_b = 0$$

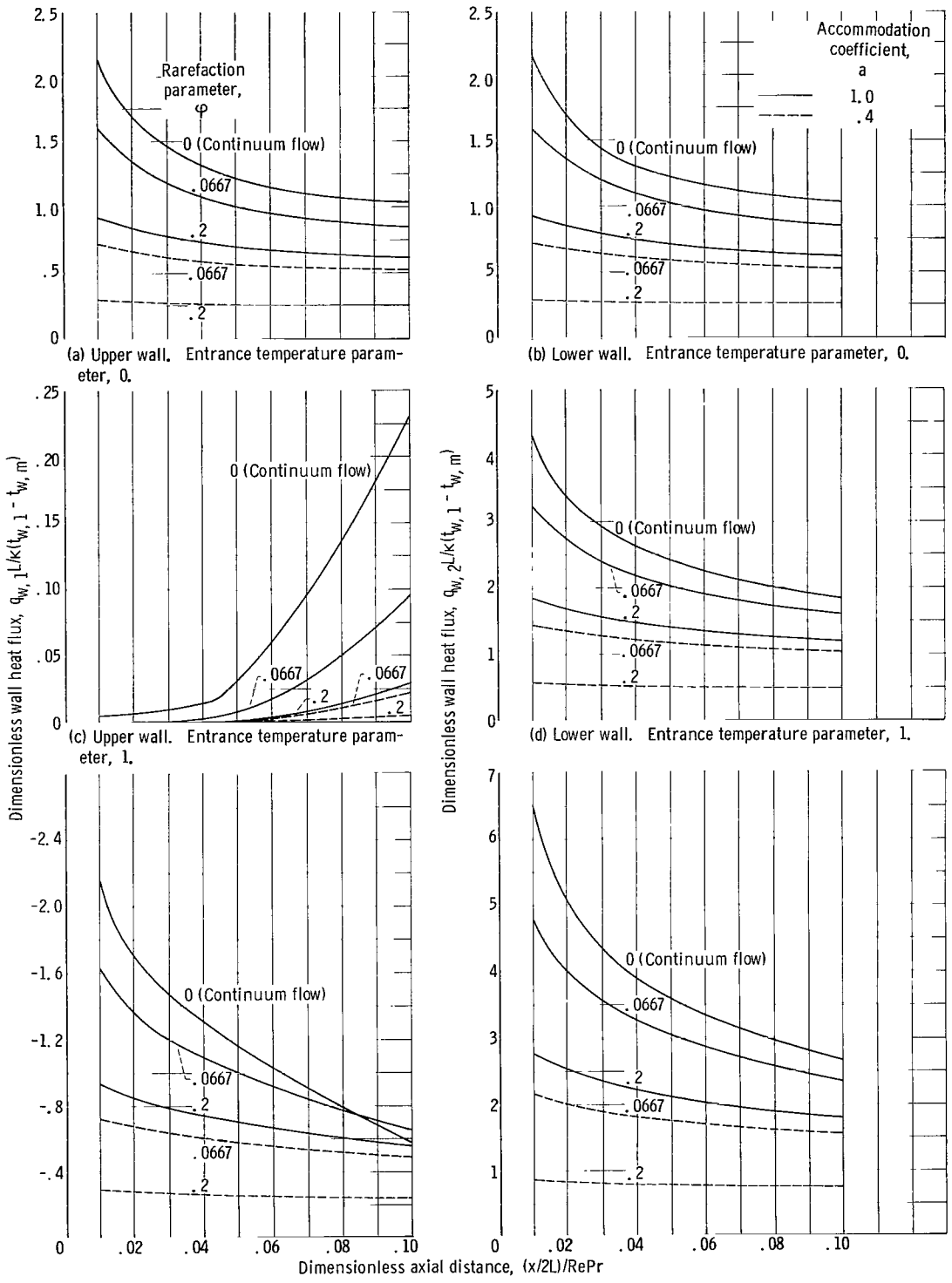

(a) Upper wall. Entrance temperature parameter, 0.

(b) Lower wall. Entrance temperature parameter, 0.

(c) Upper wall. Entrance temperature parameter, 1.

(d) Lower wall. Entrance temperature parameter, 1.

(e) Upper wall. Entrance temperature parameter, 2.

(f) Lower wall. Entrance temperature parameter, 2.

Figure 4. - Heat-flux variation in thermal entrance region. Specular reflection coefficient, 1; ratio of specific heats, 1.4; Prandtl number, 0.73.

$$Nu_1 = Nu_2 = \frac{4}{1 + 2\Gamma} + 4 \sum_{n=1}^{\infty} B_n e^{-\gamma_n \zeta}$$

and

$$T(1) = -T(-1) = \frac{1}{1 + 2\Gamma} - 2\Gamma \sum_{n=1}^{\infty} B_n e^{-\gamma_n \zeta}$$

The wall heat-flux variations required to maintain the wall temperatures constant were evaluated from equations (34) and (35) with the use of numerical values listed in tables I to IV and are plotted in figure 4 for several values of the rarefaction parameter $\varphi \equiv \mu\sqrt{R_g t}/2pL$ and the accommodation coefficient a and for the values of wall-temperature parameter T_e of 0, 1, and 2. The results for $T_e = -1$ and -2 are obtained from the figures for $T_e = 1$ and 2, respectively, by interchanging subscripts 1 and 2 on the dimensionless wall heat fluxes (e.g., $q_{w,2}L/\kappa(t_{w,1} - t_{w,m})$ for $T_e = -1$ is equal to $q_{w,1}L/\kappa(t_{w,1} - t_{w,m})$ for $T_e = 1$). For almost all cases considered, an increase in gas rarefaction produces a decrease in the heat-flux requirement, at a given axial position, over that for continuum flow, for the range of the dimensionless axial distance considered. The exception occurs for $q_{w,1}L/\kappa(t_{w,1} - t_{w,m})$ with $T_e = 2$. The accommodation coefficient a, which is generally near 1 for most surfaces and gases but which may take on much lower values for some gas-surface combinations, also has an important effect on the heat-flux variations along the channel length. Imperfect accommodation ($a \neq 1$) may substantially decrease the wall heat-flux requirements because of the increase in effective thermal contact resistance associated with the increased temperature jump. For the special case of $T_e = 0$, the heat-flux variations are the same at the two walls, with heat flowing from one wall out through the other.

The variation in Nusselt number along the channel length for each wall was evaluated from equations (44) and (45) for $T_e = 0$, 1, and 2 with the use of the numerical eigenvalues and eigenconstants from tables I to IV and is plotted in figure 5 for several values of the rarefaction parameter φ and accommodation coefficient a. The results for $T_e = -1$ and -2 are obtained from the figures for $T_e = 1$ and 2, respectively, by interchanging subscripts 1 and 2 on the Nusselt numbers.

The effect of the gas rarefaction is, in general, to decrease the Nusselt number at each wall below its continuum value at every position along the channel. For most of the cases examined the Nusselt number decreases with increasing distance from the channel entrance; however, Nu_1 for $T_e = 1$ and 2 (and therefore Nu_2 for $T_e = -1$ and -2)

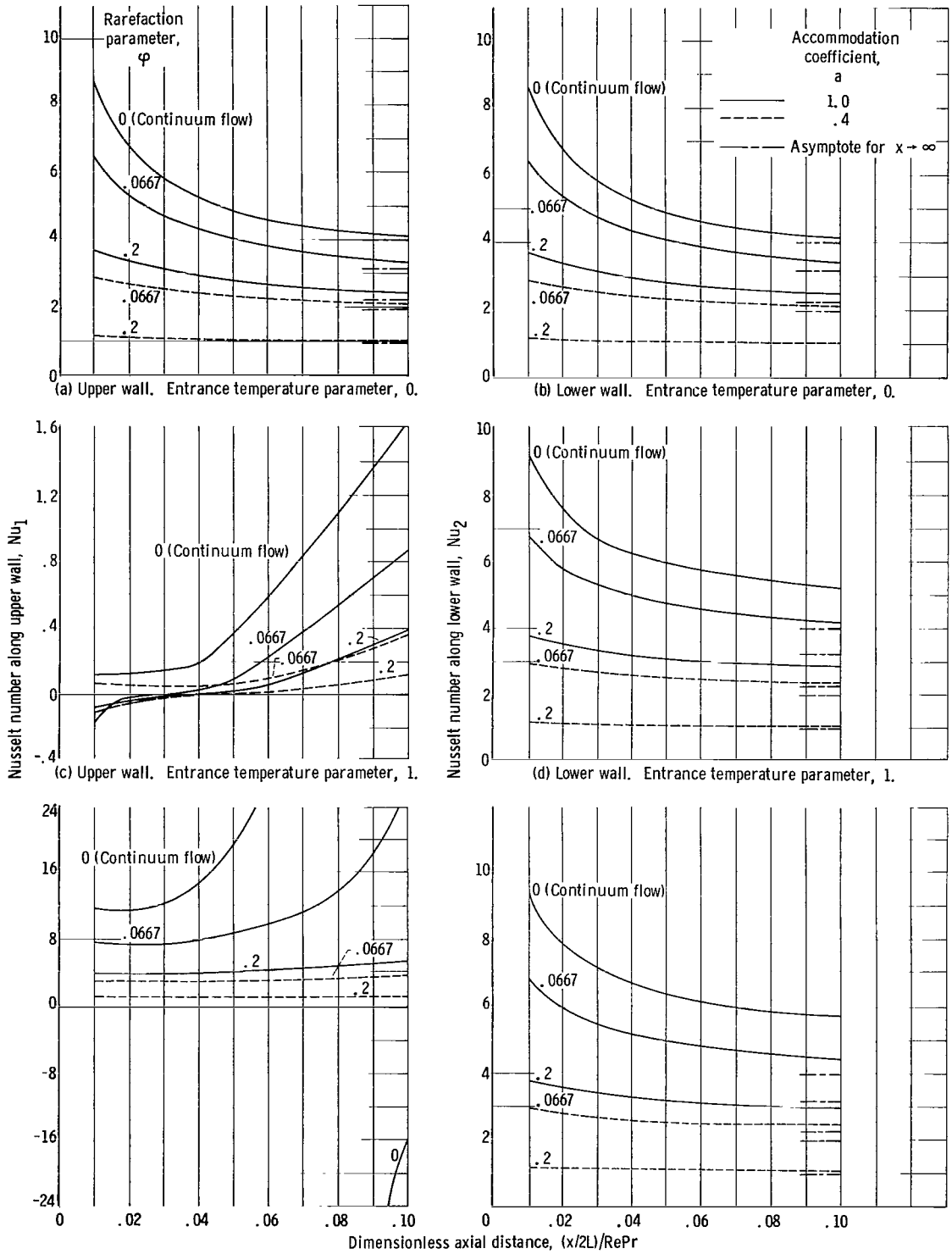

Figure 5. - Nusselt number variation in thermal entrance region. Specular reflection coefficient, 1; ratio of specific heats, 1.4; Prandtl number, 0.73.

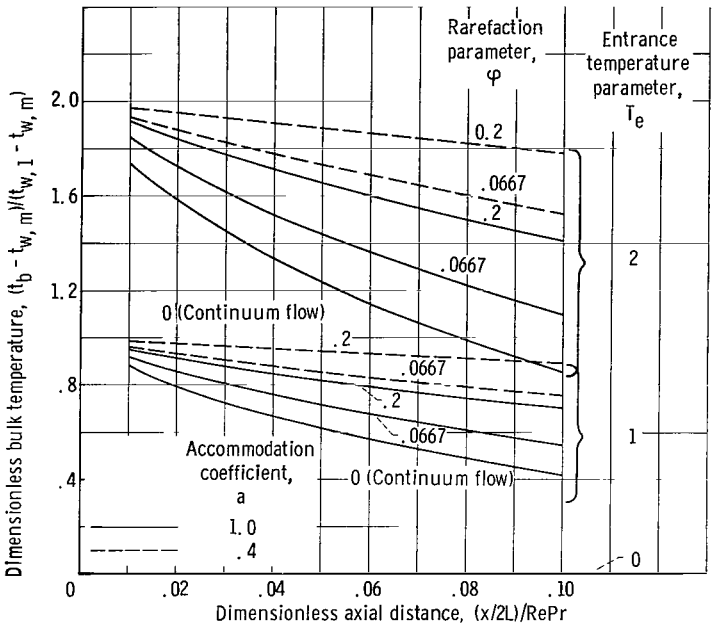

Figure 6. - Variation of gas bulk temperature for flow in parallel-plate channel. Specular reflection coefficient, 1; ratio of specific heats, 1.4; Prandtl number, 0.73.

does not follow this behavior. Infinities and zeros occur in Nu_1 if $1 \leq T_e < \infty$ and in Nu_2 if $-\infty < T_e \leq -1$. The Nusselt numbers become infinite when the bulk mean temperature of the fluid is equal to the appropriate wall temperature, that is, when $T_b = -1$ or 1 (see eqs. (43) to (45)). The longitudinal variation of the dimensionless bulk temperature T_b (eq. (43)) was examined and the results are plotted in figure 6. For $T_e = 1$ and 2 the dimensionless bulk temperature T_b commences with the value of T_e at $x = 0$ and decreases with increasing distance from the entrance. For $T_e = 0$ the dimensionless bulk temperature remains constant (equal to zero) with increasing distance from the entrance. The effect of an increase in rarefaction is to increase T_b toward the entrance value T_e at any given axial location. Imperfect accommodation increases this effect. The axial location, therefore, at which $T_b = 1$ or -1 moves downstream of the channel entrance as the gas mean free path is increased and/or the accommodation coefficient is decreased. The heat-transfer coefficient has little meaning for the situation in which the bulk mean temperature of the fluid equals the appropriate wall temperature. A thermal entrance length can be arbitrarily defined as the length of channel wall required for the Nusselt number to be within 5 percent of the fully developed value. The Nusselt number variations $Nu_1/Nu_{1,d}$ and $Nu_2/Nu_{2,d}$ in the entrance region for unequal wall temperatures were evaluated as functions of the rarefaction parameter φ and accommodation coefficient a and are presented in figure 7 for several values of the entrance temperature parameter T_e. A horizontal dashed line corresponding to an ordinate of 1.05 or an ordinate of 0.95 (depending on whether the Nusselt number ratio approaches 1 from above or below) is shown in figure 7. The case of laminar slip flow between parallel plates at equal temperatures is investigated in reference 5 and the results are included (fig. 8) for comparison. In interpreting these figures, it is important to note that the Reynolds number appears in the abscissa. For a given flow velocity and plate spacing, the Reynolds number is decreased with increased gas rarefaction. For continuum flow in a channel with unequal wall temperatures, the thermal entrance lengths are therefore very long, while the thermal entrance length at either wall is shortened with gas rarefaction. The

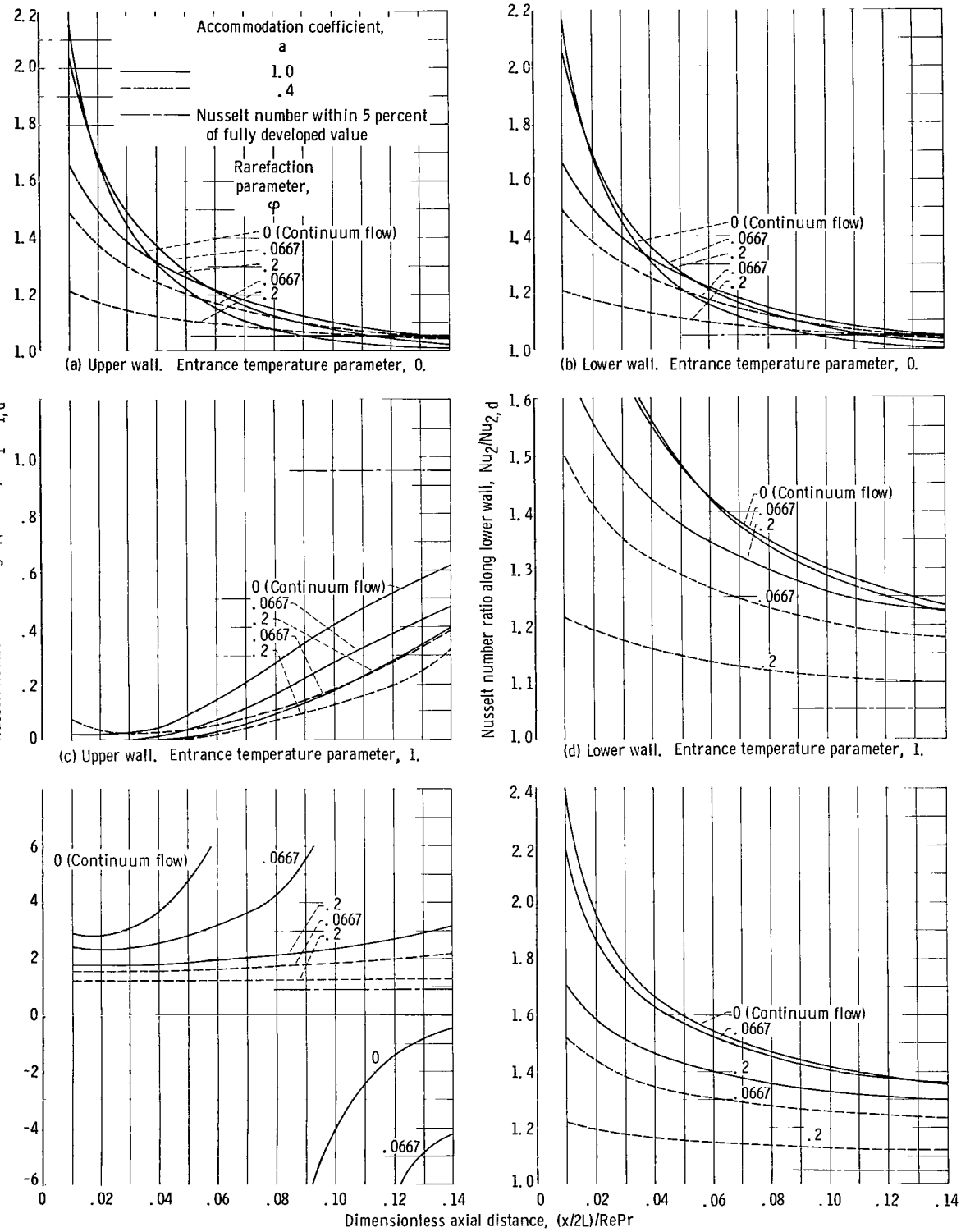

Figure 7. - Nusselt number ratio in thermal entrance region. Specular reflection coefficient, 1; ratio of specific heats, 1.4; Prandtl number, 0.73.

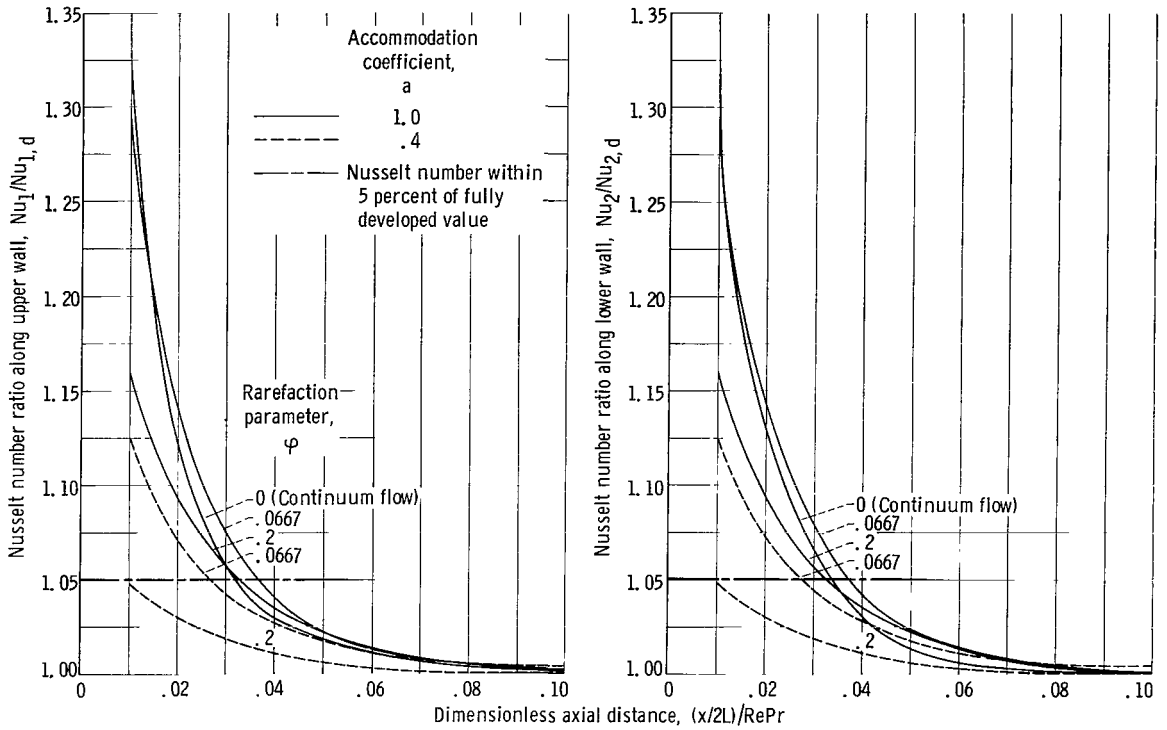

(a) Upper wall.

(b) Lower wall.

Figure 8. - Nusselt number ratio in thermal entrance region. Specular reflection coefficient, 1; ratio of specific heats, 1.4; Prandtl number, 0.73; equal wall temperatures.

increase in temperature jump with a decrease in accommodation coefficient also has an important effect on the thermal entrance length. For a given mean free path, the length required for the Nusselt number ratio to be within 5 percent of its fully developed value is least for the channel with the walls at the same temperature (fig. 8).

The variation along the length of the channel of the temperature of the gas adjacent to the upper wall and to the lower wall has been evaluated from equations (48a) and (48b), respectively, and plots are given for $T_e = 0$, 1, and 2 in figure 9. The results for $T_e = -1$ and -2 are obtained from the figures for $T_e = 1$ and 2, respectively, by interchanging subscripts 1 and 2 on the gas temperatures t_g and then multiplying the results by -1 (e.g., $T(\zeta, 1)$ for $T_e = 1$ is equal to $-T(\zeta, -1)$ for $T_e = -1$).

In the absence of rarefaction effects, the temperature of the gas adjacent to the walls changes discontinuously from the value t_e at the channel entrance ($x < 0$) to the value $t_{w,1}$ or $t_{w,2}$ at the appropriate wall and remains constant for $x \geq 0$. In other words, the difference between the surface temperature $t_{w,1}$ (or $t_{w,2}$) and the contiguous gas temperature $t_{g,1}$ (or $t_{g,2}$) is zero along the entire length of the channels. This result means that, for continuum flow, $T(\zeta, 1) = 1$ and $T(\zeta, -1) = -1$ for $x \geq 0$ for all T_e. With rarefaction, the temperature differences $t_{g,1} - t_{w,1}$ and $t_{g,2} - t_{w,2}$ have nonzero values. In general, the effect of an increase in rarefaction is to decrease $T(\zeta, 1)$ and increase $T(\zeta, -1)$ toward the entrance value T_e at any given axial location. The in-

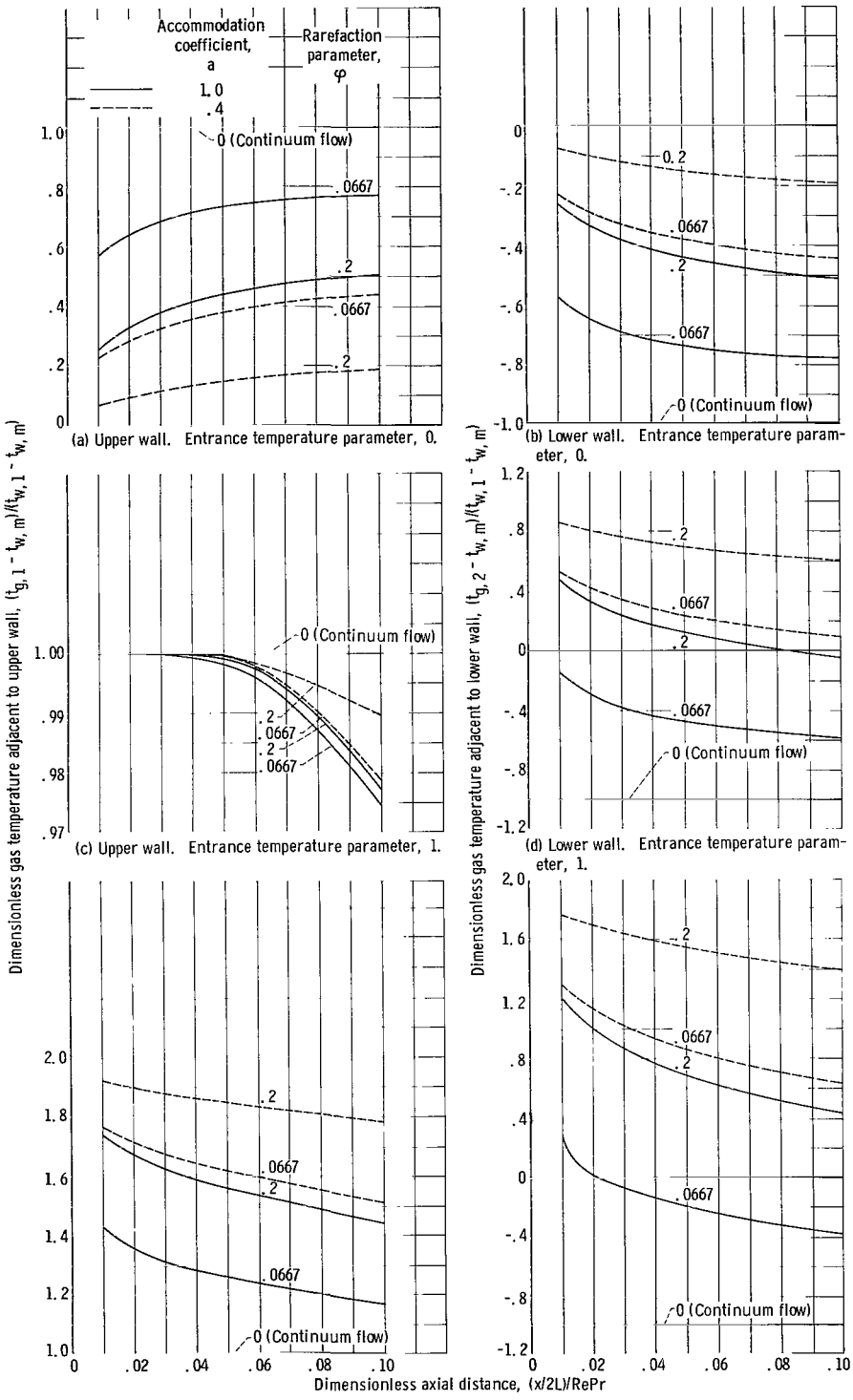

Figure 9. - Variation of gas temperature adjacent to wall. Specular reflection coefficient, 1; ratio of specific heats, 1.4; Prandtl number, 0.73.

crease in the difference between the local wall temperature and the contiguous gas temperature with an increase in accommodation coefficient is evident. The solutions for $T(\zeta, 1)$ and $T(\zeta, -1)$ approach their respective limiting values at $x \to \infty$ asymptotically for the slip flow of a gas, while for the continuum flow, there is, as mentioned previously, a step change in $T(\zeta, 1)$ and $T(\zeta, -1)$ at $x = 0$.

CONCLUSIONS

An analytical study was conducted for the laminar forced-convection heat transfer to a slightly rarefied gas flowing between two long parallel surfaces. These surfaces were taken to have constant but unequal temperatures. The wall heat fluxes and Nusselt numbers in both the entrance and the fully developed regions were obtained as functions of the gas mean free path for various values of the wall temperature constant T_e. The analysis provided analytical expressions for the even and the odd eigenvalues and eigenconstants which show good agreement with numerical results, especially for the higher eigenvalues and eigenconstants. Some of the characteristics of laminar slip flow heat transfer can be summarized as follows:

1. The wall heat-flux variation required to maintain the wall temperatures constant is, in general, decreased with an increase in gas rarefaction and/or a decrease in the value of the accommodation coefficient. The heat flux at either wall approaches asymptotically a constant value that depends solely on the temperature-jump coefficient.

2. The Nusselt numbers do not become constant until a linear temperature gradient is established in the gas, which requires, for continuum flow, fairly long entrance lengths. The Nusselt number, in general, is decreased below its continuum value because of the effect of gas rarefaction and imperfect thermal accommodation.

3. The fully developed Nusselt number is the same for either wall and is independent of the magnitude of the entrance temperature in relation to the values of the wall temperatures. It does, however, depend on the temperature-jump coefficient. The effects of gas rarefaction on the fully developed Nusselt number are more pronounced in a channel with equal wall temperatures than in a duct with unequal wall temperatures.

4. The thermal entrance length at either wall is shortened from its continuum flow value with gas rarefaction. For a given mean free path, the thermal entrance length is least for the channel with the walls at the same temperature.

Finally, other rarefaction effects, such as thermal creep velocity, would undoubtedly moderate the results given herein. Such effects were not considered in this analysis.

Lewis Research Center,
National Aeronautics and Space Administration,
Cleveland, Ohio, May 14, 1965.

APPENDIX A

SYMBOLS

A_n	coefficient defined by eq. (50)
a	accommodation coefficient
a_n	even coefficient in series expansion
a'_n	even coefficient divided by T_e, i. e., a_n/T_e
B_n	coefficient defined by eq. (64)
b_n	odd coefficient in series expansion
C	constant defined by eqs. (49) and (60)
c_p	specific heat of gas
D	arbitrary constant
D_T	thermal diameter for channel, 4L
$f(\eta)$	dimensionless velocity, $u(\eta)/\bar{u}$
G_n	coefficient in series expansion
$H(\eta)$	function of η
h	heat-transfer coefficient, $q_w/(t_w - t_b)$
I_1	definite integral defined in eq. (52)
J	indefinite integral defined in eq. (55)
J_1	definite integral defined in eq. (59), equal to I_1
L	half distance between plates
ℓ	mean free path
Nu	Nusselt number, hD_T/κ
Pr	Prandtl number, $\mu c_p/\kappa$
p	gas pressure
q_w	rate of heat transfer per unit area from wall to gas
Re	Reynolds number, $2\rho\bar{u}L/\mu$
R_g	gas constant
T	dimensionless temperature, $(t - t_{w,m})/(t_{w,1} - t_{w,m})$
T*	dimensionless entrance region temperature, $(t - t_d)/(t_{w,1} - t_{w,m})$
t	gas temperature
t_g	temperature of gas adjacent to wall
$t_{w,m}$	temperature equal to arithmetic average of wall temperatures, $(t_{w,1} + t_{w,2})/2$
$u(\eta)$	gas velocity
$\bar{u}$	average velocity
$X(\zeta)$	function of ζ
x	axial coordinate
Y	even transverse distribution function
Y_n	even eigenfunctions of eqs. (21)
y	transverse coordinate
Z	odd transverse distribution function

Z_n odd eigenfunctions of eqs. (21)

Z_ν odd eigenfunctions of eq. (B3)

α dimensionless velocity-slip coefficient, $\xi_u/2L$

β separation constant

β_n even eigenvalues of eqs. (21)

Γ dimensionless temperature-jump coefficient, $\xi_t/2L$

γ separation constant

γ_n odd eigenvalues of eqs. (21)

γ_ν odd eigenvalues of eq. (B3)

δ_n $\sqrt{\beta_n}\, I_1$

ϵ_n $\sqrt{\gamma_n}\, J_1$

ζ dimensionless axial distance, $4(x/2L)/RePr$

η dimensionless transverse coordinate, y/L

κ gas thermal conductivity

λ ratio of specific heats

μ gas viscosity

ξ_t temperature-jump coefficient

ξ_u velocity-slip coefficient

ρ gas density

σ specular reflection coefficient

φ rarefaction parameter, $\mu\sqrt{R_g t}/2pL$

ψ separation constant

Subscripts:

b gas bulk condition

d fully developed region or condition

e entrance, x = 0

g gas adjacent to wall

s slip

w wall

0 continuum flow conditions

1 upper wall, y = L

2 lower wall, y = -L

APPENDIX B

EVALUATION OF SERIES COEFFICIENTS b_n

The odd coefficients of the series expansion (eq. (26)) are determined as the quotient of two integrals (eq. (25)):

$$b_n = -\frac{\frac{1}{1+2\Gamma}\int_0^1 \eta f(\eta) Z_n(\eta) d\eta}{\int_0^1 f(\eta) Z_n^2(\eta) d\eta} \tag{25}$$

With equation (21a) applied to the odd eigenfunctions $Z_n(\eta)$, the integral appearing in the numerator may be written as

$$\int_0^1 \eta f(\eta) Z_n(\eta) d\eta = -\frac{1}{\gamma_n}\int_0^1 \eta \frac{d^2 Z_n}{d\eta^2} d\eta$$

$$= -\frac{1}{\gamma_n}\left\{\left[\left(\eta \frac{dZ_n}{d\eta}\right)\right]_0^1 - \int_0^1 \frac{dZ_n}{d\eta} d\eta\right\}$$

$$= -\frac{1}{\gamma_n}\left(\frac{dZ_n}{d\eta}\right)_{\eta=1} + \frac{1}{\gamma_n} Z_n(1) \tag{B1}$$

since $Z_n(0) = 0$. According to equation (21b), however,

$$Z_n(1) = -2\Gamma\left(\frac{dZ_n}{d\eta}\right)_{\eta=1}$$

so that

$$\int_0^1 \eta f(\eta) Z_n(\eta) d\eta = -\frac{1+2\Gamma}{\gamma_n}\left(\frac{dZ_n}{d\eta}\right)_{\eta=1} \tag{B2}$$

In order to evaluate the integral in the denominator of equation (25), let Z_ν and Z_n be the solutions associated with two distinct values of γ: γ_ν and γ_n. Therefore,

$$\frac{d^2Z_\nu}{d\eta^2} + \gamma_\nu f(\eta)Z_\nu = 0 \qquad \text{with } Z_\nu(1) = -2\Gamma\left(\frac{dZ_\nu}{d\eta}\right)_{\eta=1} ; \; Z_\nu(0) = 0 \tag{B3}$$

and

$$\frac{d^2Z_n}{d\eta^2} + \gamma_n f(\eta)Z_n = 0 \qquad \text{with } Z_n(1) = -2\Gamma\left(\frac{dZ_n}{d\eta}\right)_{\eta=1} ; \; Z_n(0) = 0 \tag{B4}$$

Equation (B3) is multiplied by Z_n and equation (B4) by Z_ν, and then equation (B4) is subtracted from (B3). The result, after transposing, is

$$(\gamma_n - \gamma_\nu)f(\eta)Z_\nu Z_n = -\frac{d}{d\eta}\left(Z_\nu \frac{dZ_n}{d\eta} - Z_n \frac{dZ_\nu}{d\eta}\right)$$

If this equation is integrated between 0 and 1, the following is obtained:

$$(\gamma_n - \gamma_\nu)\int_0^1 f(\eta)Z_\nu Z_n \, d\eta = -\left(Z_\nu \frac{dZ_n}{d\eta} - Z_n \frac{dZ_\nu}{d\eta}\right)\Bigg|_0^1 \tag{B5}$$

where $Z_\nu(\eta, \gamma_\nu)$ and $Z_n(\eta, \gamma_n)$ for $\nu \neq n$ are orthogonal functions with respect to the weight function $f(\eta)$; that is,

$$\int_0^1 f(\eta)Z_\nu Z_n \, d\eta = 0 \qquad \text{for} \qquad \nu \neq n \tag{B6}$$

This property of the eigenfunctions was used in obtaining equation (25).

If $\gamma_\nu = \gamma_n$, the integral on the left side of equation (B5) becomes the integral of the square of the characteristic function:

$$\int_0^1 f(\eta)Z_n^2(\eta)d\eta = -\lim_{\nu \to n} \frac{\left(Z_\nu \frac{dZ_n}{d\eta} - Z_n \frac{dZ_\nu}{d\eta}\right)\Big|_0^1}{\gamma_n - \gamma_\nu}$$

The expression on the right assumes the intermediate form 0/0. Hence, it is necessary to apply L'Hospital's rule and to differentiate numerator and denominator with respect to γ_ν before setting $\gamma_\nu = \gamma_n$. Carrying out this differentiation results in

$$\int_0^1 f(\eta)Z_n^2(\eta)d\eta = \left(\frac{\partial Z_n}{\partial \eta}\frac{\partial Z_n}{\partial \gamma_n} - Z_n\frac{\partial^2 Z_n}{\partial \eta\,\partial \gamma_n}\right)\Bigg|_0^1 = \left(\frac{\partial Z_n}{\partial \eta}\frac{\partial Z_n}{\partial \gamma_n}\right)_{\eta=1}$$

$$- \left(Z_n\frac{\partial^2 Z_n}{\partial \eta\,\partial \gamma_n}\right)_{\eta=1} - \left(\frac{\partial Z_n}{\partial \eta}\frac{\partial Z_n}{\partial \gamma_n}\right)_{\eta=0} \qquad \text{(B7)}$$

Near $\eta \sim 0$, the boundary condition $Z_n(0) = 0$ requires that the odd solution to equation (21a) be given by $Z_n(\eta \sim 0) = F \sin\left(\sqrt{\gamma_n f(0)}\eta\right)$, where F is an arbitrary constant. Hence, at $\eta = 0$,

$$\left(\frac{\partial Z_n}{\partial \eta}\right)_{\eta=0} = F\sqrt{\gamma_n f(0)}$$

$$\left(\frac{\partial Z_n}{\partial \gamma_n}\right)_{\eta=0} = 0$$

Thus, equation (B7) reduces to

$$\int_0^1 f(\eta)Z_n^2(\eta)d\eta = \left(\frac{\partial Z_n}{\partial \eta}\frac{\partial Z_n}{\partial \gamma_n} - Z_n\frac{\partial^2 Z_n}{\partial \eta\,\partial \gamma_n}\right)_{\eta=1} \qquad \text{(B8)}$$

Into this expression, there is now substituted the boundary condition

$$Z_n(1) = -2\Gamma\left(\frac{dZ_n}{d\eta}\right)_{\eta=1}$$

This substitution gives

$$\int_0^1 f(\eta) Z_n^2(\eta) d\eta = \left(\frac{\partial Z}{\partial \gamma} + 2\Gamma \frac{\partial^2 Z}{\partial \eta \, \partial \gamma} \right)_{\eta=1;\, \gamma=\gamma_n} \left(\frac{\partial Z_n}{\partial \eta} \right)_{\eta=1} \tag{B9}$$

Therefore using equations (25), (B2), and (B9) yields

$$b_n = \frac{1}{\gamma_n \left(\frac{\partial Z}{\partial \gamma} + 2\Gamma \frac{\partial^2 Z}{\partial \eta \, \partial \gamma} \right)_{\eta=1;\, \gamma=\gamma_n}} \tag{B10}$$

REFERENCES

1. Yih, C. S.; and Cermak, Jack E.: Laminar Heat Convection in Pipes and Ducts. Rept. No. 5, Civil Eng. Dept., Colorado College of Agricultural and Mech. Arts, Sept. 1951.

2. Schenk, J.; and Beckers, H. L.: Heat Transfer in Laminar Flow Between Parallel Plates. Appl. Sci. Res., sec. A, vol. 4, no. 1, 1953-1954, pp. 405-413.

3. Cess, R. D.; and Shaffer, E. C.: Summary of Laminar Heat Transfer Between Parallel Plates with Unsymmetrical Wall Temperatures. Jour. Aero/Space Sci., vol. 26, no. 8, Aug. 1959, p. 538.

4. Hatton, A. P.; and Turton, J. S.: Heat Transfer in the Thermal Entry Length With Laminar Flow Between Parallel Walls at Unequal Temperatures. Int. J. Heat and Mass Transfer, vol. 5, 1962, pp. 673-679.

5. Inman, Robert M.: Heat Transfer for Laminar Slip Flow of a Rarefied Gas in a Parallel-Plate Channel or a Circular Tube with Uniform Wall Temperature. NASA TN D-2213, 1964.

6. Inman, Robert M.: Laminar Slip Flow Heat Transfer in a Parallel-Plate Channel or a Round Tube with Uniform Wall Heating. NASA TN D-2393, 1964.

7. Schaaf, S. A.; and Chambre, P. L.: Flow of Rarefied Gases. Princeton Univ. Press, 1961, pp. 9; 34.

8. Carslaw, H. S.; and Jaeger, J. C.: Conduction of Heat in Solids. Second ed., Oxford Clarendon Press, 1959, pp. 491; 492.

9. Dzung, L. S.: Heat Transfer in a Flat Duct with Sinusoidal Heat Flux Distribution. Proc. Second U. N. Conf. on Peaceful Uses of Atomic Energy (Geneva), vol. 7, 1958, pp. 671-675.

3/1/25

"The aeronautical and space activities of the United States shall be conducted so as to contribute . . . to the expansion of human knowledge of phenomena in the atmosphere and space. The Administration shall provide for the widest practicable and appropriate dissemination of information concerning its activities and the results thereof."

—NATIONAL AERONAUTICS AND SPACE ACT OF 1958

NASA SCIENTIFIC AND TECHNICAL PUBLICATIONS

TECHNICAL REPORTS: Scientific and technical information considered important, complete, and a lasting contribution to existing knowledge.

TECHNICAL NOTES: Information less broad in scope but nevertheless of importance as a contribution to existing knowledge.

TECHNICAL MEMORANDUMS: Information receiving limited distribution because of preliminary data, security classification, or other reasons.

CONTRACTOR REPORTS: Technical information generated in connection with a NASA contract or grant and released under NASA auspices.

TECHNICAL TRANSLATIONS: Information published in a foreign language considered to merit NASA distribution in English.

TECHNICAL REPRINTS: Information derived from NASA activities and initially published in the form of journal articles.

SPECIAL PUBLICATIONS: Information derived from or of value to NASA activities but not necessarily reporting the results of individual NASA-programmed scientific efforts. Publications include conference proceedings, monographs, data compilations, handbooks, sourcebooks, and special bibliographies.

Details on the availability of these publications may be obtained from:

SCIENTIFIC AND TECHNICAL INFORMATION DIVISION

NATIONAL AERONAUTICS AND SPACE ADMINISTRATION

Washington, D.C. 20546